

Chaotic signature of climate extremes

Ibiyinka FUWAPE · Sunday
OLUYAMO · Babatunde RABIU ·
Samuel OGUNJO

Received: date / Accepted: date

Abstract Understanding the dynamics of climate extreme is important in its prediction and modeling. In this study, linear trends in percentile, threshold, absolute, and duration based temperature and precipitation extremes indicator were obtained for the period 1979 - 2012 using the ETCCDI data set. The pattern of trend was compared with nonlinear measures (Entropy, Hurst Exponent, Recurrence Quantification Analysis) of temperature and precipitation. Regions which show positive trends in temperature based extremes were found to be areas with low entropy and chaotic. Complexity measures also revealed that the dynamics of the southern hemisphere differs from that of the northern hemisphere.

Keywords climate extremes · chaos · recurrence quantification analysis

Ogunjo S. T. acknowledges funding and support from the Max Planck Institute for the Physics of Complex Systems

I. Fuwape, S. Oluyamo
Department of Physics, Federal University of Technology, Akure
Ondo State, Nigeria.
E-mail: iafuwape@futa.edu.ng, ssoluyamo@futa.edu.ng
Present address: of I. Fuwape
Michael and Cecilia Ibru University, Ughelli, Delta State, Nigeria.

B. Rabi
Centre for Atmospheric Research
National Space Research and Development Agency,
Anyigba, Kogi State, Nigeria.

S. T. Ogunjo
Department of Physics, Federal University of Technology, Akure
Ondo State, Nigeria.
E-mail: stogunjo@futa.edu.ng, ogunjo@pks.mpg.de.

1 Introduction

The impact of climate change will be felt in varying degrees in different parts of the world. Global mean surface temperature was reported to rise about $0.6^{\circ}C$ in the last century and expected to rise between $1.4 - 5.8^{\circ}C$ in the next century (Boo et al 2006). The observed trends in climate time series can either be deterministic (external forcing) or stochastic (intrinsic variability) (Franzke 2011). At the regional level where intrinsic climate variability play a great role, climate extremes in temperature and precipitation have significant impact in our agriculture, health, energy, ecosystem and society (Schoof and Robeson 2016). A set of indices, for monitoring of climate extremes based on temperature and precipitation data, has been defined by the Expert Team on Climate Change Detection and Indices (ETCCDI). The ease of use and interpretation of the defined indices have made it useful for the study of global extreme events (Sillman et al 2013; Alexander et al 2006) and for regions (Schoof and Robeson 2016; Alexander and Arblaster 2017; Boo et al 2006; Klein Tank and Konnen 2003). Climate change is expected to modify the characteristics of extreme weather and climate events (Abiodun et al 2017). For instance, increasing warm and decreasing cool temperature based indices have been reported for Australia (Collins et al 2000) and Southeast Asia (Manton et al 2001), increase of about 3% per decade in short duration extreme precipitation events in the United States (Kunkel et al 1999) and increased occurrence of extreme temperature over Nigeria (Abiodun et al 2013; Abatan et al 2017).

According to Sivakumar (2004), it is important to investigate complexity in geophysical phenomena for short and long term predictions, model testing and better description of the phenomena. The development of nonlinear techniques and their robust performance over linear methods have led to an increase in the search for structures and understanding of complexity in geophysical phenomena in recent times Sivakumar et al (2007). Detecting chaos is more complicated in time series than in flows and discrete dynamical systems. Graphical methods of identifying chaotic systems includes phase space reconstruction, poincare section, close return plot, and recurrence plot. New measures of complexity have been introduced based on structures in a recurrence plot (Zbilut and Webber 2015). Complexity and level of chaos can be estimated by computing the dimension and entropy of the system (Rosenstein et al 1993). The sensitivity of a system to initial conditions can be determined by the Lyapunov exponents. A system with at least one positive Lyapunov exponent is regarded as being chaotic. Different algorithms for computing the Lyapunov exponent has been proposed by Rosenstein et al (1993), Sano and Sawada (1985), Kantz (1994) and Wolf et al (1985). Other methods of identifying chaotic systems include the method of surrogate data (Theiler et al 1992), 0 – 1 test (Gottwald et al 2004) and delay vector variance (Fuwape and Ogunjo 2016; Gautama et al 2004). Chaos investigation has been conducted into precipitation data (Fuwape et al 2017; Kyoung et al 2011; Sivakumar et al 2006); temperature data (Fuwape et al 2017; Millán et al 2010), wind speed data (An et al 2012; Samet and Marzbani 2014) and solar radiation

data (Ogunjo et al 2017). The presence of noise, large number of zeros, and data size has been cited as limitations to the use of nonlinear techniques. The presence of zeros was deemed to be less severe when compared to presence of noise and data size in the application of nonlinear techniques to other fields (Sivakumar et al 2006). In the study of climate over a period of thirty years, the data length is sufficient for extraction of features (Sivakumar 2005).

In the case of El Niño Southern Oscillation (ENSO), the discussion is about whether a deterministic or stochastic model best describes it. Rejection of chaos in the time series of ENSO has been disputed based on analysis carried out using Largest Lyapunov Exponent (Kawamura et al 1998), Correlation Dimension (Kawamura et al 1998), close return plots (Ahn and Kim 2005) and determinism (Binder and Wilches 2012). The theory that ENSO time series is a stochastic system rather than a chaotic one has led to the development of stochastic approach for ENSO (Ubilava and Helmers 2013; Hall et al 2001). Several studies have identify chaos in the dynamics of ENSO using tools such as bred vector (Tang and Deng 2010), dynamical models (Vallis 1986; Chang et al 1996; Tziperman et al 1994), false nearest neighbour and correlation dimension (Chang et al 1996; Tsonis 2009), Lyapunov Exponent (Tsonis 2009) and nonlinear prediction error (Elsner and Tsonis 1993). The dimension of ENSO reported from dynamical models include 3.5 (Tziperman et al 1994), 2.4 & 2.6 (Chang et al 1996), < 2 (Jin et al 2005), 3 and 4 (Tsonis 2009) and 8 (Aijain 1998). The possibility of co-existing chaotic dynamics in the seasonal dynamics and stochastic dynamics in the interannual timing and strength of ENSO (Zivkovic and Rypdal 2013) and noise induce chaotic dynamics (Stone et al 1998) has been proposed.

It has been posited that our climate system is both chaotic and complex (Rind 1999). For example, ENSO has been shown to influence river flow in the tropics and subtropics (Khan et al 2006) and Asian irrigation has remote impact on African rainfall (de Vrese et al 2016). The effect of changing climate in one region on or in relation to another region can only be studied on a global rather than regional level. While several studies have indicated chaos in geophysical phenomena at local level, the dynamics of our changing climate needs to be investigated on the global scale. To this end, this study aims to investigate the chaotic signature of climate change by comparing dynamical analysis of temperature and precipitation to observed trend across the world.

2 Data

2.1 Data

The indices described by the ETCCDI (Klein Tank et al 2009) can be categorized into percentile based indices, absolute indices, threshold indices, duration indices and other indices (Alexander et al 2006). An index was chosen in each category for both temperature and precipitation as shown in Table 1. Annual values of all ETCCDI indices have been computed for various data sets (global

Table 1 List of extreme precipitation and temperature indices as defined by the ETCCDI (Sillman et al 2013) used in this study

| Index | Label | Definition |
|--------------------------|--------|---|
| Extremely wet days | R99p | Annual precipitation derived from days > 99th percentile |
| Max. 1-day precipitation | RX1day | Maximum 1-day precipitation |
| Heavy precipitation days | R10mm | Annual count of days with precipitation > 10 mm |
| Consecutive wet days | CWD | Max. number of consecutive days with precipitation > 1 mm |
| Simple daily index | SDII | Mean precipitation amount on wet days |
| Warm days | TX90p | Percentage of days with T_{max} > historical 90th percentile value |
| Maximum T_{min} | TNx | Maximum value of T_{min} |
| Summer days | SU | Number of days with $T_{max} > 25^{\circ}C$ |
| Warm spell duration | WSDI | Annual count of at least six consecutive days with T_{max} > the historical 90th percentile value |
| Diurnal range | DTR | Mean difference between daily T_{max} and T_{min} |

climate models, observational data and reanalyses) using consistent methodologies (Sillman et al 2013). Computed values of indices for the ERA-Interim reanalysis data set from 1979 - 2012 were retrieved from the ETCCDI indices archive at www.cccma.ec.gc.ca/data/climdex/climdex.shtml. Linear trends in the climatic extremes over 34 years were taken as the linear regression coefficient.

In order to ensure consistency and uniformity, data for computation of nonlinear measures were also obtained for daily precipitation and minimum temperature data from the ERA-Interim reanalysis studies (Dee et al 2011) from 1979 - 2012 on a regular $1.5^{\circ} \times 1.5^{\circ}$ grid. However, data processing such as removal of outliers and consecutive equal values control were not carried out on the data. Approaches to removal of trends have been shown to have effect on computed nonlinear measures (Ogunjo 2015), hence, precipitation and minimum temperature anomalies were used for nonlinear analysis.

3 Methodology

3.1 Entropy

Entropy is regarded as a measure of disorder in a system. In thermodynamics, entropy is the degree of disorder in a system, in information theory, it is the amount of information obtainable from a system while in statistical mechanics, entropy is the number of microscopic state of a system in thermodynamic equilibrium. The concept of entropy has been extended as a measure of complexity in a time series. The Boltzmann-Gibbs entropy is defined as

$$S_i = - \sum_{i=1}^W p_i \ln(p_i) \quad (1)$$

where W is the number of macroscopically indistinguishable microscopic configurations (Singh 1997). Tsallis (1988) defined entropy for nonextensive system as

$$S_q = \frac{k}{q-1} \left(1 - \sum_{i=1}^W p_i^q \right) \quad (2)$$

where p_i are the probabilities associated with the microscopic configurations, W is their total number, q is a real number, and k is Boltzmann's constant (Kalimeri et al 2008). In the limit $q \rightarrow 1$, Tsallis entropy (equation 2) becomes the Boltzmann-Gibbs entropy (equation 1). Entropy analysis has been used in the spatio-temporal dynamics of tropical climate (Fuwape et al 2017), delineation of water resources zones in Japan (Kawachi et al 2001), pre-seismic emissions (Kalimeri et al 2008), investigation of abrupt climate change in Earth's climate (Gonzalez et al 2011) and application in hydrological processes (Singh 1997).

3.2 Hurst Exponent

Given a time series Z , the average $X(\tau)$ and standard deviation $S(\tau)$ of the sequence of observations are computed as Equation 3 and 4 respectively (where τ is the time lag).

$$X(\tau) = \sum_{u=1}^t (Z(u) - \langle Z \rangle_\tau) \quad (3)$$

$$S(\tau) = \left(\frac{1}{\tau} \sum_{t=1}^{\tau} (Z(t) - \langle Z \rangle_\tau)^2 \right)^{\frac{1}{2}} \quad (4)$$

Defining the self adjusted range as

$$R(\tau) = \max_{t=1}^{\tau} \{X(\tau)\} - \min_{t=1}^{\tau} \{X(\tau)\} \quad (5)$$

Hurst exponent, H is then computed from the expression $\log(R/S) = \log(\tau/2)^H$ (Fuwape and Ogunjo 2016). Persistence, anti-persistence, and uncorrelated processes are indicated by $0.5 < H < 1$, $0 < H < 0.5$ and $H = 0.5$ respectively. Hurst exponent has been applied to precipitation and river runoff records using DFA (Kantelhardt et al 2006), annual precipitation in the United States using Rescale Range method (Potter 1979) and other time series (Fuwape and Ogunjo 2016).

3.3 Recurrence Quantification Analysis (RQA)

Marwan et al (2007) defined the recurrence of a system $R_{i,j}$ at time i in a different time j as

$$R_{i,j}^{m,\epsilon_i} = \theta(\epsilon_i - \|\mathbf{x}_i - \mathbf{x}_j\|) \quad (6)$$

where ϵ_i , $\|\cdot\|$, θ are the threshold for distance, Euclidean norm and Heaviside function respectively (Panagoulia and Vlahogianni 2014). Recurrence plots have small scale structures which can be used to quantify complexity. Three of these measures, known as recurrence quantification analysis will be employed in this study: Recurrence rate (REC), Determinism (DET) and Divergence (DIV). REC is defined as the density of recurrence points, DET is the ratio of recurrence points that form diagonal structures to all recurrence points and DIV is the inverse of the longest diagonal line in the recurrence plot. Relationship between RQA parameters and measures such as Lyapunov exponent, correlation dimension and Renyi entropy has been reported in literature (Marwan et al 2007; Zbilut and Webber 2006). In this study, the threshold is taken as $\epsilon > 5\sigma$. Recurrence plots and recurrence quantification analysis have been employed in several climate studies (Panagoulia and Vlahogianni 2014).

4 Results and discussion

In this section, the results of linear trends in temperature and precipitation trends, as well as chaotic analysis carried out as described in Section 3, on minimum temperature, maximum temperature and precipitation data are presented and discussed.

4.1 Linear trend in extreme temperature and precipitation indices

Figure 1 shows the trend in temperature based extremes over the globe in the period 1979 - 2012. Over terrestrial land surface, the percentile based index, TX90p showed a decreasing trend in the northern coast of South America, southern America, southern Asia, western Australia and Canada. Continental warming could be seen in the central regions of South America and Africa. Over the Ocean, the El Nino region in the Pacific showed decreasing trend while warming could be observed in the Atlantic and Indian Oceans. The absolute index, TNx showed decreasing trends with varying intensity across the tropics, central Europe and continental North America. It also showed warming in Antarctica and the Arctic region. The number of summer days (SU) showed warming in the Mediterranean sea and Europe. Across the tropics, cooling could be observed in both land and sea surface with regions of warming in the northern and southern regions of both Pacific and Atlantic oceans. Warm spell duration (WSDI) showed similar trend to the percentile index (TX90p), albeit with a lesser degree of intensity. The world oceans, central regions of South America and Africa showed increasing trend in diurnal temperature range. The greatest decrease in DTR were found in Southern Africa and Asia. The results obtained show significant similarity with other global (Christidis and Stott 2016; Hansen et al 2010; Vose et al 2005) and regional (Chou et al 2014) reports.

The percentile (R99p) and absolute (RX1day) indices showed similar trend (Figure 2). Notable trends were found in central Africa, northern region of

South America and Pacific islands. While a decreasing linear trend was observed in central Africa, an increasing trend was found in northern region of South America. The threshold based index (R10mm) and duration based index (CWD) revealed changes in tropical region. Along the tropics, a cooling trend was observed in the R10mm index and a warming trend in the northern regions of South America and Pacific Islands. Similar but more noticeable pattern was observed in the CWD index.

4.2 Complexity in global temperature and precipitation

Figures 3 and 4 showed the computed nonlinear signatures of minimum and maximum temperature respectively using the method of Tsallis Entropy, Hurst Exponent and Recurrence Quantification Analysis (RQA). The Tsallis Entropy of minimum temperature revealed a high degree of disorderliness or randomness over most of the land. The entropy values are much higher for northern and southern Africa, most of Asia, Australia and northern region of North America than Europe and southern region of North America. Lower entropy values were observed for the central region of both South America, Africa and tropical Asia. Surfaces of the ocean reveal a different dynamics as the tropical regions of the oceans show a lower entropy value than surrounding ocean body. This is more obvious in the Tsallis entropy value of maximum temperature (Figure 4). Both land and ocean in the tropics show lower entropy values than the surrounding areas. The increasing entropy with increasing latitude seen over West Africa has also been reported by Fuwape et al (2017).

The computed Hurst Exponent for both minimum and maximum temperatures show identical features. Most of the global land mass show persistence (i.e. an increasing (decreasing) trend will be followed by an increasing (decreasing) trend). These values are, however, lower than that obtained over the ocean. The Hurst exponent values in the El nino region shows $1/f$ noise while regions in the Atlantic ocean show low values of Hurst Exponent. Regions in the central part of South America and Africa showed values different from global trends.

Low values of recurrence rates shows that minimum temperature over the oceans are chaotic except for the western coast of both South America and Atlantic Ocean. The highest value of recurrence rate were observed in the Arctic Ocean. Australia shows a chaotic values in minimum temperature which reduces towards the equator. Land mass along the tropics including the islands in the Pacific Oceans shows chaotic trend while continental land mass tend towards stochastic values. From the map of divergence, the chaotic nature of minimum and maximum temperature could be ascertained. Low dimensional chaos could be found in minimum and maximum temperature across continental land mass. This result could explain the low predictability reported in the El nino region and Pacific islands using observational data (Hunt and Dix 2017).

In the Pacific ocean, predominant low entropy values were interspersed by narrow streams of high entropy values below and above the El nino regions. The low entropy values observed in the Pacific ocean does not translate into low entropy values in continental North and South America, although streaks of high entropy values transverse longitudinally through the central North America. Contrary to the low entropy values obtained for minimum and entropy values in central regions of South America and Africa, high entropy values were found for precipitation data in those regions. Similarly, while high entropy values obtained for minimum and maximum temperature in northern Africa and Australia, the regions showed low entropy values for precipitation. The low entropy values in the Australian continent belongs to the stream of high entropy values observed in the Tropic of Capricorn.

Precipitation showed persistence across the tropics. The spread seems to weaken as it moves from the Pacific ocean, through central South America into the Atlantic Ocean. Incoherent patterns of uncorrelated precipitation could be observed across the globe. In the northern hemisphere, precipitation showed random walk in northern Africa, parts of Europe, Asia and North America.

The dynamics of precipitation across the globe was investigated using recurrence rate, determinism and divergence. The same trend of results were observed across the three quantifiers with recurrence rate showing more distinct features than determinism and divergence. Most of the continental land mass showed chaotic behaviour with low recurrence rates with the exception of regions in northern Africa, Australia, Yemen and Oman. The **stochastic** nature of precipitation in the Arabian sea did not follow the chaotic trend observed in the Indian ocean. The region from the Indian ocean through the Pacific islands to the Indian ocean were also found to exhibit chaotic precipitation. In the El nino region, the chaotic region gave way to two pitchfork surrounding a **non-chaotic** region. **Non-chaotic** values of precipitation were found along the Tropic of Capricorn with more intensity in the Pacific and Indian Oceans. In the Atlantic ocean, the coast of West Africa and northern Africa also exhibit **non-chaotic** behaviours.

4.3 Relationship between trends of extreme climate and complexity measures

The footprint of precipitation extremes could not be observed in the global isoentropy or chaos map but the signature of temperature based extremes could be found around the globe. This suggests that solar activity is the main large-scale driver of deterministic chaos across the globe (Faranda et al 2017). This position is further strengthened by the different patterns of results in the northern and southern hemisphere. The differences observed between the northern and southern hemisphere have been attributed to difference in absorbed solar radiation, difference in outgoing long wave radiation and cross-equatorial heat transport (Feulner et al 2013). The net surface heat flux has been found to account for the sea surface temperature variability over the southern hemisphere (Reason 2000).

Considering trends in temperature climate extremes (Figures 1) and corresponding complexity measures in minimum and maximum temperature (Figure 3 and 4), similarities could be observed between linear trends in DTR and TX90p, and Tsallis entropy for land areas. Regions with positive trends in DTR corresponds to regions with lower entropy. These regions include central regions of both South America and Africa and eastern coast of Asia. Across the tropics, the region off the coast of South America with negative trend in TX90p show corresponding chaoticity (low recurrence rate) while positive trend in the tropical Atlantic Ocean and Equatorial region show high recurrence rate. However, the cooling observed in TX90p in the Southern mid-latitude did not result in low recurrence rate. This can be attributed to the role of ocean dynamics (Gille 2002; Reason 2000).

5 Summary and concluding remarks

We have studied the global spatial trend in temperature extremes (TX90p, TNx, SU, WSDI and DTR) and precipitation extremes (R90p, RX1day, R10mm, CWD and SDII). The results obtained showed varying degrees of cooling and warming across the earth with enhanced activity in the ENSO and tropical region. Similarly, the dynamical complexities were investigated using Tsallis Entropy, Hurst Exponent, and Recurrence Quantification Analysis (RQA). While the footprint of precipitation extremes could not be observed in the analysis, positive trend in temperature extremes were found in regions which show low entropy and chaos. Furthermore, the nonlinear analysis of temperature also revealed the different dynamics of both northern and southern hemisphere, which confirms previous studies. While we have studied global spatial dynamics of temperature and precipitation, there is the need for temporal studies to understand the evolution of climate phenomena.

Acknowledgements Part of this research was carried out at the Max Planck Institute for the Physics of Complex Systems, Dresden, Germany by Ogunjo Samuel.

References

- Abatan AA, Abiodun BJ, Gutowski Jr WJ, Razaq-Balogun SO (2017) Trends and variability in absolute indices of temperature extremes over nigeria: linkage with nao. *International Journal of Climatology* In Press, DOI 10.1002/joc.5196
- Abiodun BJ, Lawal KA, Salami AT, Abatan AA (2013) Potential influences of global warming on future climate and extreme events in nigeria. *Regional Environmental Change* 13(3):477–491
- Abiodun BJ, Adegoke J, Abatan AA, Ibe CA, Egbebiyi TS, Engelbrecht F, Pinto I (2017) Potential impacts of climate change on extreme precipitation over four african coastal cities. *Climate Change* 143:399–413
- Ahn JH, Kim HS (2005) Nonlinear modeling of el nino/southern oscillation index. *Journal of Hydrological Engineering* 10(1):8–15
- Aijain CM (1998) Characterizing enso with nonlinear dynamics. Msc., University of Rhode Island

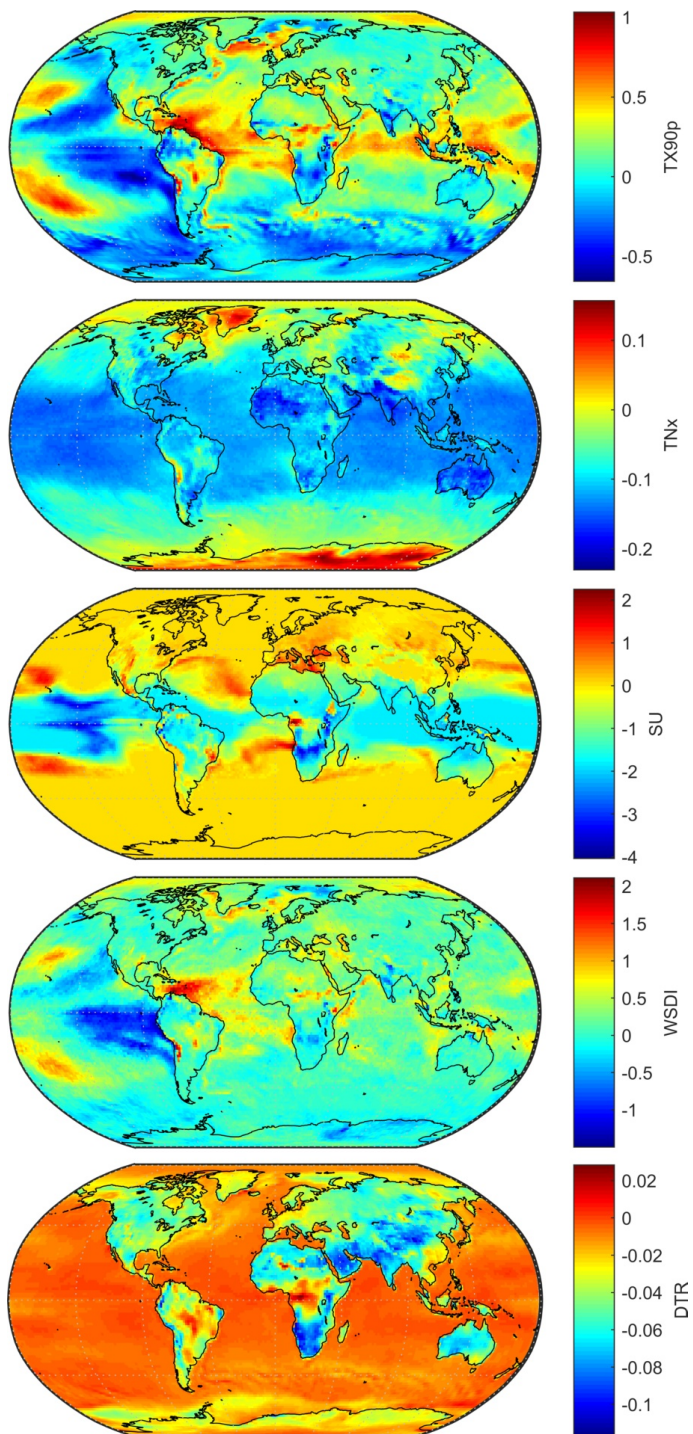


Fig. 1 Trends in temperature indices (from top to bottom) TX90p, TNx, SU, WSDI and DTR

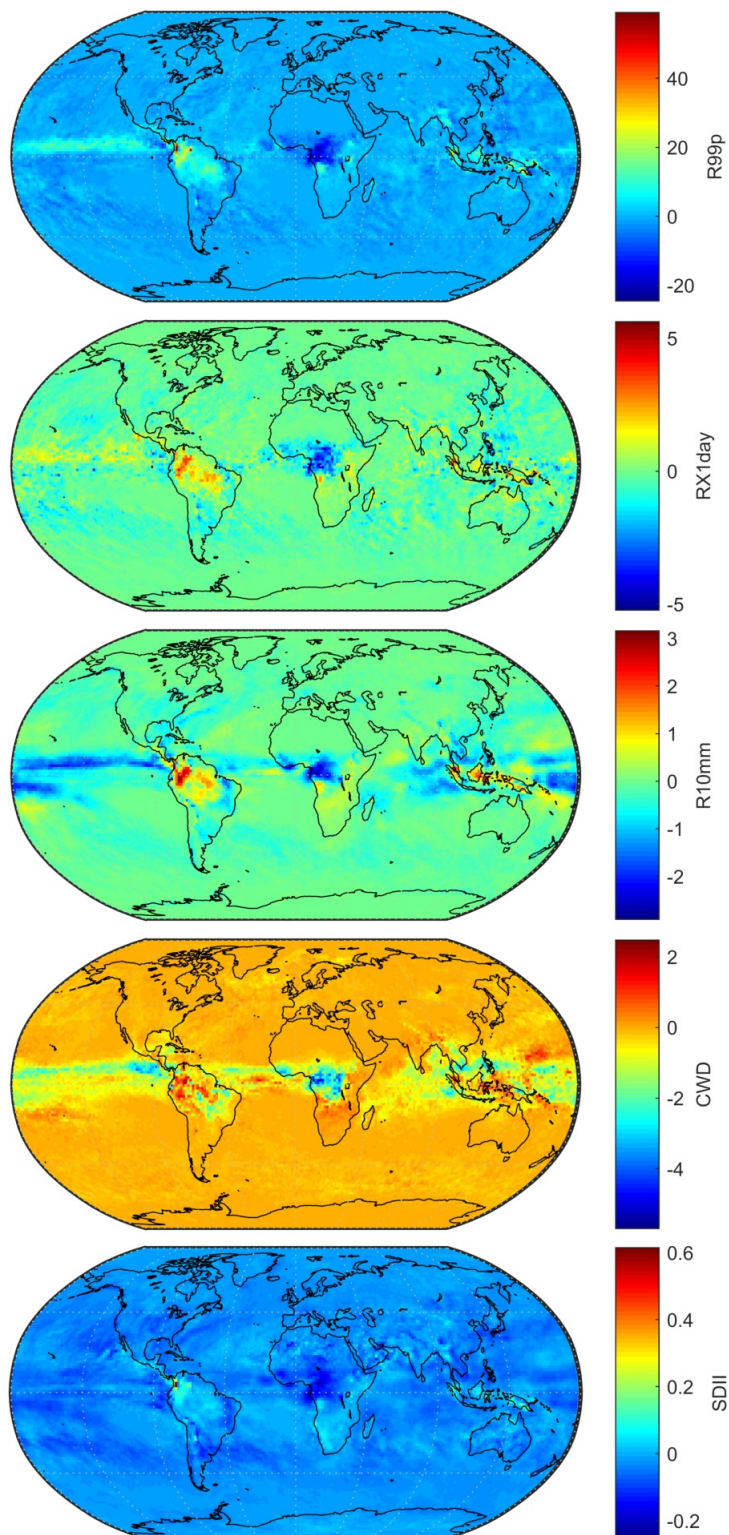


Fig. 2 Trends in precipitation indices (from top to bottom) R90p, RX1day, R10mm, CWD and SDII

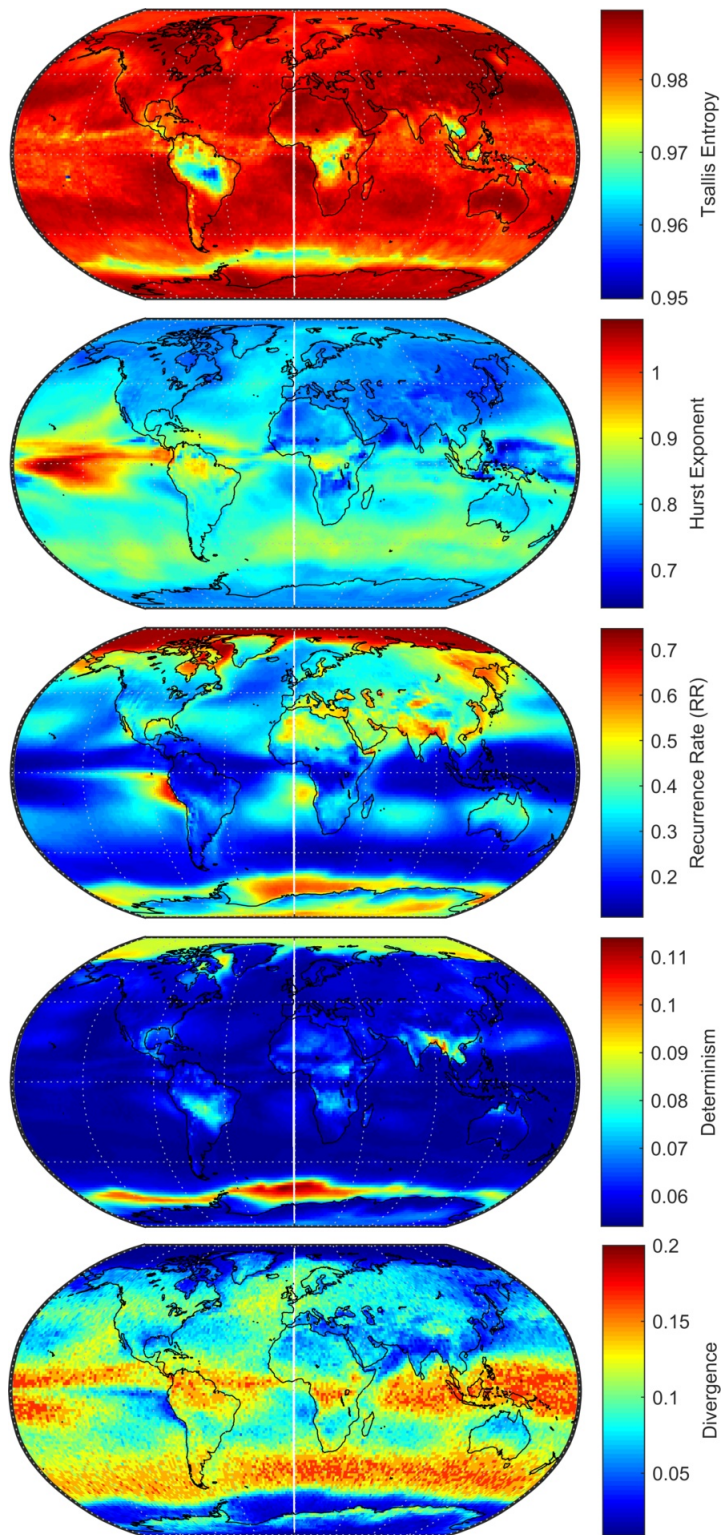


Fig. 3 Complexity measures for minimum temperature using (from top to bottom) Tsallis entropy, Hurst Exponent, Recurrence Rate, Determinism, Divergence

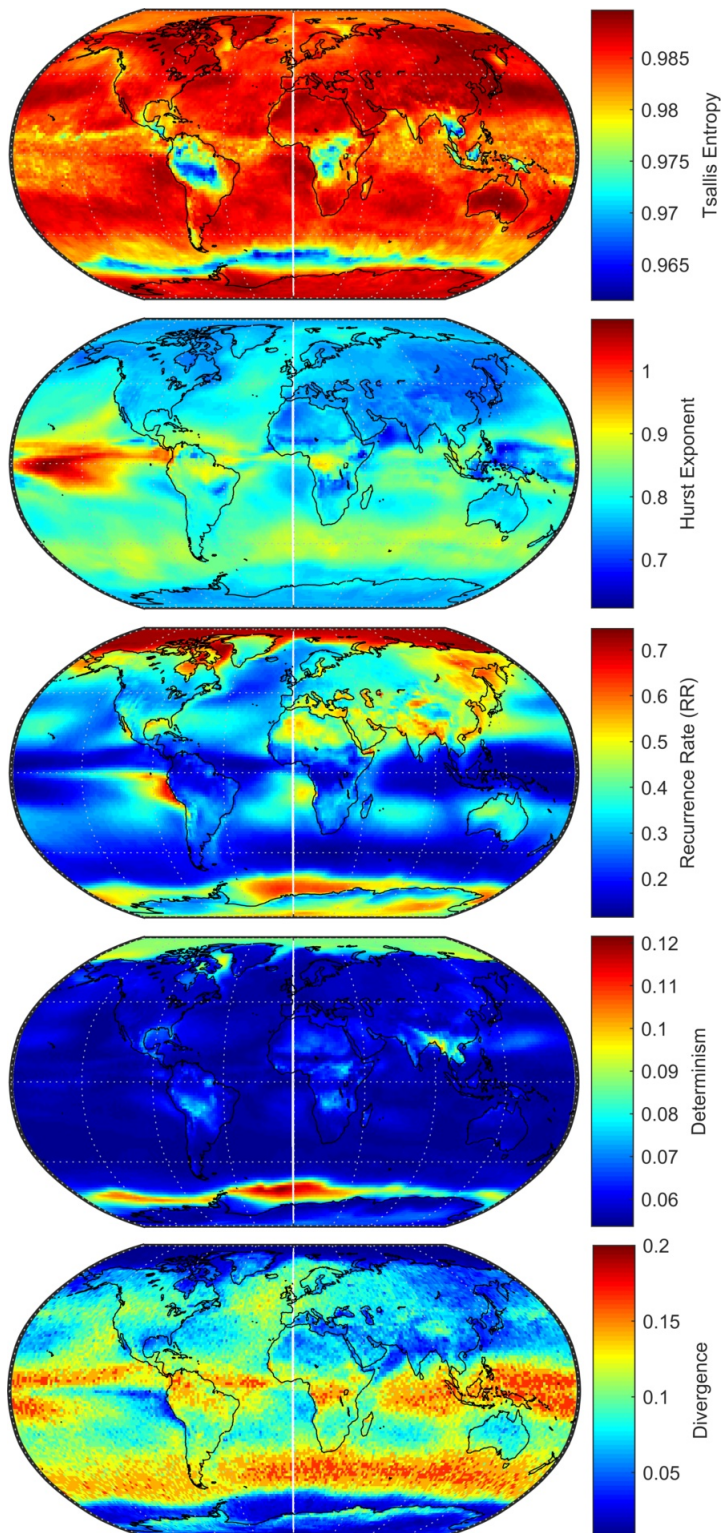


Fig. 4 Same as in Figure 3 but for maximum temperature

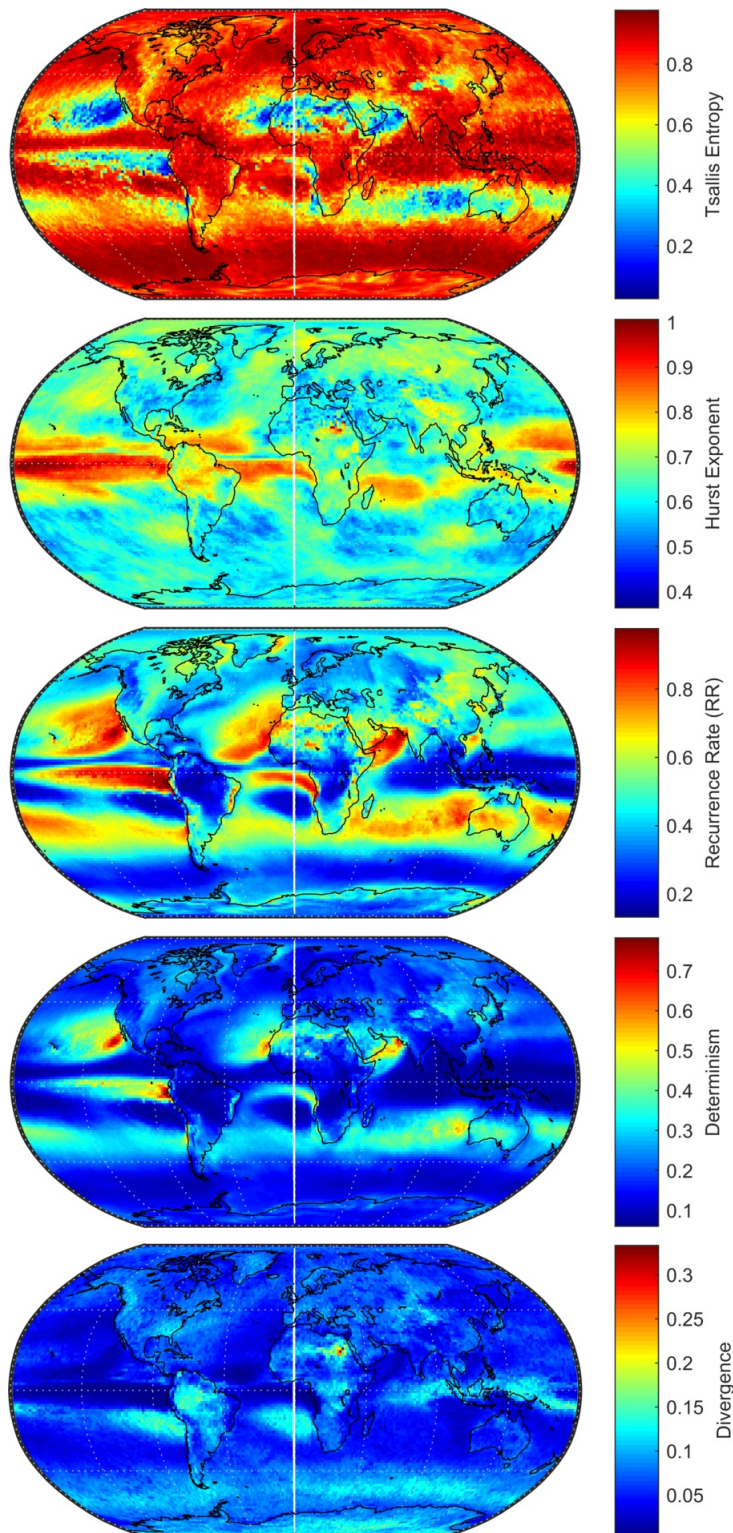


Fig. 5 Same as in Figure 3 but for precipitation

- Alexander L, Arblaster JM (2017) Historical and projected trends in temperature and precipitation extremes in australia in observations and cmip5. *Weather and Climate Extremes* 15:34–56
- Alexander LV, Zhang X, Peterson TC, Caesar J, Gleason B, Klein Tank AMG, Haylock M, Collins D, Trewin B, Rahimzadeh F, Tagipour A, Rupa Kumar K, Revadekar J, Griffiths G, Vincent L, Stephenson DB, Burn J, Aguilar E, Brunet M, Taylor M, New M, Zhai P, Rusticucci M, Vazquez-Aguirre JL (2006) Global observed changes in daily climate extremes of temperature and precipitation. *Journal of Geophysical Research: Atmospheres* 111(D5):D05109, DOI 10.1029/2005JD006290, URL <http://dx.doi.org/10.1029/2005JD006290>
- An X, Jiang D, Zhao M, Liu C (2012) Short term prediction of wind power using emd and chaotic theory. *Commun Nonlinear Sci Numer Simul* 17:1036–1042
- Binder P, Wilches CA (2012) Absence of determinism in el nino southern oscillation. *Physical Review E* 65:055207
- Boo K, Kwon W, Baek H (2006) Change of extreme events of temperature and precipitation over korea using regional projection of future climate change. *Geophysical Research Letters* 33:L01701
- Chang P, Ji L, Li H, Flugel M (1996) Chaotic dynamics versus stochastic processes in el nino - southern oscillation in coupled ocean-atmosphere models. *Physica D* 98:301–320
- Chou SC, Lyra A, Mourão C, Derczynski C, Pilotto I, Gomes J, Bustamante J, Tavares P, Silva A, Rodrigues D, et al (2014) Evaluation of the eta simulations nested in three global climate models. *American Journal of Climate Change* 3(5):438–454
- Christidis N, Stott PA (2016) Attribution analyses of temperature extremes using a set of 16 indices. *Weather and Climate Extremes* 14:24–35, URL <http://www.sciencedirect.com/science/article/pii/S2212094716300640>
- Collins DA, Della-Marta PM, Plummer N, Trewin BC (2000) Trends in annual frequencies of extreme temperature events in australia. *Aust Met Mag* 49:277–292
- de Vrese P, Hagemann S, Claussen M (2016) Asian irrigation, african rain: Remote impacts of irrigation. *Geophysical Research Letters* 43(8):3737–3745
- Dee DP, Uppala SM, Simmons AJ, Berrisford P, Poli P, Kobayashi S, Andrae U, Balmaseda MA, Balsamo G, Bauer P, Bechtold P, Beljaars ACM, Berg LVD, Bidlot J, Bormann N, Delsol C, Dragani R, Fuentes M, Geer AJ (2011) The ERA-Interim reanalysis : configuration and performance of the data assimilation system. *Q J R Meteorol Soc* 137(656):553–597, DOI 10.1002/qj.828
- Elsner JB, Tsonis AA (1993) Nonlinear dynamics established in the enso. *Geophysical Research Letters* 20(2):213–216
- Faranda D, Messori G, Alvarez-Castro MC, Yiou P (2017) Dynamical properties and extremes of northern hemisphere climate fields over the past 60 years. *Nonlin Processes Geophys*, 24:713–725
- Feulner G, Rahmstorf S, Levermann A, Volkwardt S (2013) On the origin of the surface air temperature difference between the hemispheres in earth’s present-day climate. *Journal of Climate* 26(18):7136–7150, URL <https://doi.org/10.1175/JCLI-D-12-00636.1>
- Franzke C (2011) Nonlinear trends, long-range dependence, and climate noise properties of surface temperature. *Journal of Climate* 25:4172
- Fuwape IA, Ogunjo ST (2016) Quantification of scaling exponents and dynamical complexity of microwave refractivity in a tropical climate. *J Atmos Solar-Terrestrial Phys* 150-151:61–68, DOI 10.1016/j.jastp.2016.10.010
- Fuwape IA, Ogunjo ST, Oluyamo SS, Rabiun AB (2017) Spatial variation of deterministic chaos in mean daily temperature and rainfall over nigeria. *Theoretical and Applied Climatology* 130(1):119–132, DOI 10.1007/s00704-016-1867-x, URL <https://doi.org/10.1007/s00704-016-1867-x>
- Gautama T, Mandic DP, Hulle MMV (2004) The delay vector variance method for detecting determinism and nonlinearity in time series. *Phys D* 190:167–176, DOI 10.1016/j.physd.2003.11.001
- Gille ST (2002) Warming of the southern ocean since the 1950s. *Science* 295(5558):1275–1277, DOI 10.1126/science.1065863, URL <http://science.sciencemag.org/content/295/5558/1275>, <http://science.sciencemag.org/content/295/5558/1275.full.pdf>

- Gonzalez J, de Faria E, Albuquerque MP, Albuquerque MP (2011) Nonadditive Tsallis entropy applied to the Earth's climate. *Phys A Stat Mech its Appl* 390(4):587–594, DOI 10.1016/j.physa.2010.10.045
- Gottwald GA, Melbourne I, A PRSL (2004) A new test for chaos in deterministic systems pp 603–611, DOI 10.1098/rspa.2003.1183
- Hall AD, Skalin J, Terasvirta T (2001) A nonlinear time series model of el nino. *Environmental Modelling & Software* 16:139–146
- Hansen J, Ruedy R, Sato M, Lo K (2010) Global surface temperature change. *Reviews of Geophysics* 48(4):n/a–n/a, DOI 10.1029/2010RG000345, URL <http://dx.doi.org/10.1029/2010RG000345>, rG4004
- Hunt BG, Dix MR (2017) Stochastic implications for long-range rainfall predictions. *Climate Dynamics* DOI 10.1007/s00382-017-3572-6, URL <https://doi.org/10.1007/s00382-017-3572-6>
- Jin Y, Kawamura A, Jinno K, Berndtsson R (2005) Nonlinear multivariate analysis of soi and local precipitation and temperature. *Nonlinear Processes in Geophysics* 12:67–74
- Kalimeri M, Papadimitriou C, Balasis G, Eftaxias K (2008) Dynamical complexity detection in pre-seismic emissions using nonadditive Tsallis entropy. *Phys A Stat Mech its Appl* 387(5-6):1161–1172, DOI 10.1016/j.physa.2007.10.053
- Kantelhardt JW, Koscielny-Bunde E, Rybski D, Braun P, Bunde A, Havlin S (2006) Long-term persistence and multifractality of precipitation and river runoff records. *J Geophys Res Atmos* 111(1):D01,106, DOI 10.1029/2005JD005881, URL <http://doi.wiley.com/10.1029/2005JD005881>
- Kantz H (1994) A robust method to estimate the maximal Lyapunov exponent of a time series. *Phys Lett A* 185(1):77–87
- Kawachi T, Maruyama T, Singh VP (2001) Rainfall entropy for delineation of water resources zones in japan. *Journal of Hydrology* 246(1-4):36–44
- Kawamura A, McKerchar AI, Spigel RH, Jinno K (1998) Chaotic characteristics of the southern oscillation index time series. *Journal of Hydrology* 204:168–181
- Khan S, Ganguly AR, Bandyopadhyay S, saigal S, Erickson III DJ, Protopoulos V, Ostrochov G (2006) Nonlinear statistics reveals stronger ties between enso and the tropical hydrological cycle. *Geophysical Research Letters* 33:L24,402
- Klein Tank AMG, Konnen GP (2003) Trends in indices of daily temperature and precipitation extremes in europe, 1946-99. *Journal of Climate* 16:3665
- Klein Tank AMG, Zwiers FW, Zhang X (2009) Guidelines on analysis of extremes in a changing climate in support of informed decisions for adaptation, climate data and monitoring. Tech. Rep. WCDMP-No 72, World Meteorological Organization, wMO-TD No. 1500
- Kunkel KE, Andsageer K, Easterling DR (1999) Long term trends in extreme precipitation events over the conterminous united states and canada. *Journal of Climate* 12:2515–2528
- Kyoung MS, Kim HS, Sivakumar B, Singh VP, Ahn KS (2011) Dynamic characteristics of monthly rainfall in the Korean Peninsula under climate change. *Stoch Environ Res Risk Assess* 25(4):613–625, DOI DOI10.1007/s00477-010-0425-9
- Manton M, Della-Marta P, Haylock M, Hennessy K, Nicholls N, Chambers L, Collins D, Daw G, Finet A, Gunawan D, Inape K, Isobe H, Kestin T, Lefale P, Leyu C, Lwin T, Maitrepierre L, Ouprasitwong N, Page C, Pahalad J, Plummer N, Salinger M, Suppiah R, Tran V, Trewin B, Tibig I, Yee D (2001) Trends in extreme daily rainfall and temperature in southeast asia and the south pacific: 1961?1998. *International Journal of Climatology* 21(3):269–284, DOI 10.1002/joc.610, URL <http://dx.doi.org/10.1002/joc.610>
- Marwan N, Romano MC, Thiel M, Kurths J (2007) Recurrence plots for the analysis of complex systems. *Physics Reports* 438(5-6):237–329
- Millán H, Ghanbarian-Alavijeh B, Garcia-Fornaris I (2010) Nonlinear dynamics of mean daily temperature and dewpoint time series at Balolsar, Iran, 1961 - 2005. *Atmos Res* 98(1):89–101, DOI 10.1016/j.atmosres.2010.06.001
- Ogunjo S (2015) Effect of Data Transformation on Long Term Memory of Chaotic Time Series. *African Rev Phys* 10:219–224
- Ogunjo ST, Adediji AT, Dada JB (2017) Investigating chaotic features in solar radiation over a tropical station using recurrence quantification analysis. *Theor Appl Climatol* 127(1-2):421–427, DOI 10.1007/s00704-015-1642-4

- Panagoulia D, Vlahogianni EI (2014) Nonlinear dynamics and recurrence analysis of extreme precipitation for observed and general circulation model generated climates. *Hydrological Processes* 28(4):2281–2292, DOI 10.1002/hyp.9802, URL <http://doi.wiley.com/10.1002/hyp.9802>
- Potter KW (1979) Annual precipitation in the northeast united states: Long memory, short memory or no memory? *Water Resources Research* 15(2):340–347
- Reason CJC (2000) Multidecadal climate variability in the subtropics/mid-latitudes of the southern hemisphere oceans 52A:203–223
- Rind D (1999) Complexity and climate. *Science* 284(5411):105–107
- Rosenstein MT, Collins JJ, de Luca CJ (1993) A practical method for calculating largest Lyapunov exponents from small data sets. *Phys D Nonlinear Phenom* 65(1–2):117–134, URL <http://www-anw.cs.umass.edu/~mtr/papers/RosensteinM93.pdf>
- Samet H, Marzbani F (2014) Quantizing the deterministic nonlinearity in wind speed time series. *Renew Sustain Energy Rev* 39:1143–1154, DOI 10.1016/j.rser.2014.07.130
- Sano M, Sawada Y (1985) Measurement of the Lyapunov Spectrum from a Chaotic Time Series. *Phys Rev Lett* 55(10):1082–1085, DOI 10.1103/PhysRevLett.55.1082, URL <http://link.aps.org/doi/10.1103/PhysRevLett.55.1082>
- Schoof JT, Robeson SM (2016) Projecting changes in regional temperature and precipitation extremes in the united states. *Weather and Climate Extremes* 11:28–40
- Sillman J, Kharin VV, Zhang X, Zwiers FW, Bronaugh D (2013) Climate extremes indices in the cmip5 multimodel ensemble: Part 1. model evaluation in the present climate. *Journal of Geophysical Research: Atmospheres* 118:1716–1733
- Singh VP (1997) The use of entropy in hydrology and water resources. *Hydrological Processes* 11:587–626
- Sivakumar B (2004) Chaos theory in geophysics: past, present and future. *Chaos Solitons & Fractals* 19(2):441–462, DOI 10.1016/s0960-0779(03)00055-9
- Sivakumar B (2005) Correlation dimension estimation of hydrological series and data size requirement : myth and reality. *Hydrological Science* 50(4):591–603, DOI 10.1623/hysj.2005.50.4.591
- Sivakumar B, Wallender WW, Horwath WR, Mitchell JP, Prentice SE, Joyce Ba (2006) Nonlinear analysis of rainfall dynamics in California’s Sacramento Valley. *Hydrological Processes* 20(December 2005):1723–1736, DOI 10.1002/hyp.5952
- Sivakumar B, Jayawardena AW, Li WK (2007) Hydrologic complexity and classification: a simple data reconstruction approach. *Hydrological Processes* 21:2713–2728
- Stone L, Saparin PI, Huppert A, Price C (1998) El nino chaos: The role of noise and stochastic resonance on the enso cycle. *Geophysical Research Letters* 25(2):175–178
- Tang Y, Deng Z (2010) Low dimensional nonlinearity of enso and its impact on predictability. *Physica D* 239:258–268
- Theiler J, Eubank S, Longtin A, Galdrikian B, Farmer JD (1992) Testing for nonlinearity in time series: the method of surrogate data. *Physica D* 58:77–94
- Tsallis C (1988) Possible generalization of boltzmann-gibbs statistics. *J Stat Phys* 52:479
- Tsonis AA (2009) Dynamical changes in the enso system in the last 11000 years. *Climate Dynamics* 33:1069
- Tziperman E, Stone L, Cane MA, Jarosh H (1994) El nino chaos: Overlapping of resonances between the seasonal cycle and the pacific ocean-atmosphere oscillator. *Science* 264:72–74
- Ubilava D, Helmers CG (2013) Forecasting enso with a smooth transition autoregressive model. *Environmental Modelling & Software* 40:181–190
- Vallis GK (1986) El nino: A chaotic dynamical system? *Science* 232:243
- Vose RS, Easterling DR, Gleason B (2005) Maximum and minimum temperature trends for the globe: An update through 2004. *Geophysical Research Letters* 32(23):n/a–n/a, DOI 10.1029/2005GL024379, URL <http://dx.doi.org/10.1029/2005GL024379>, l23822
- Wolf A, Swift JB, Swinney HL, Vastano, Vastano JA (1985) Determining Lyapunov exponents from a time series. *Phys D Nonlinear Phenom* 16(3):285–317, DOI 10.1093/rof/rfs003
- Zbilut JP, Webber CL (2006) Recurrence Quantification Analysis. In: *Wiley Encycl. Biomed. Eng.*, John Wiley & Sons, Inc., Hoboken, NJ, USA, DOI 10.1002/9780471740360.

-
- ebs1355, URL <http://doi.wiley.com/10.1002/9780471740360.ebs1355>
- Zbilut JP, Webber CL (2015) Recurrence Quantification Analysis. JANUARY, DOI 10.1007/978-3-319-07155-8, URL <http://link.springer.com/10.1007/978-3-319-07155-8>
- Zivkovic T, Rypdal K (2013) Enso dynamics: Low dimensional chaotic or stochastic? *Journal of Geophysical Research* 118:2161–2168